BNL-105151-2014-TECH

Booster Technical Note No. 107;BNL-105151-2014-IR

Closed orbit analysis for the AGS Booster

J. Milutinovic

February 1988

Collider Accelerator Department

Brookhaven National Laboratory

U.S. Department of Energy

USDOE Office of Science (SC)

DISCLAIMER

CLOSED ORBIT ANALYSIS FOR THE AGS BOOSTER

AD
Booster Technical Note
No. 107

J. MILUTINOVIC AND A. G. RUGGIERO

FEBRUARY 1, 1988

ACCELERATOR DEVELOPMENT DEPARTMENT
Brookhaven National Laboratory
Upton, N.Y. 11973

Abstract

We examine the effects of four types of errors in the AGS Booster dipoles and quadrupoles on the on-momentum closed orbit in this machine. We use PATRIS both to handle statistically the effects of kick-modeled errors and to check the performance of the Fermilab correcting scheme in a framework of a more realistic modeling. For the latter to be effective, we find that the r.m.s. values of the errors should not go much beyond 3×10^{-4} in the appropriate units.

Introduction

An accelerator lattice cannot be expected to be perfect, just as anything else made by man. Fortunately, there are theorems which guarantee the existence of a closed orbit even in an imperfect lattice, provided the deviations from the ideal lattice are not too big. However, large ranges of existing closed orbits will actually be of no value, because such closed orbits might violate aperture and other limitations and therefore be unacceptable. Hence, from the practical point of view, it is of utmost importance to determine both qualitative and quantitative links between the lattice imperfections and the resulting closed orbits. In this note we have addressed this important issue and have estimated the limitations on some of the lattice imperfections for the closed orbit to be correctable. The types of imperfections that we have handled are the dipole integrated field strength error $\Delta(Bl)/Bl$, the dipole axial rotation $\Delta\theta$, and the quadrupole lateral displacements in both planes. In this procedure it is very important that the same error is assigned to one physical magnet even if the magnet is divided in two or more parts. PATRIS now does this error assigning in the correct manner.

Statistical Treatment of Closed Orbit Errors in the Kick Approximation

For the purpose of quick statistical treatment of the effects of magnet imperfections on the closed orbit, PATRIS employs an algorithm whose basic ingredients are given in the Courant-Snyder paper[1]. The starting point is the equation of motion for the transverse degrees of freedom

$$\frac{d^2y}{ds^2} + K(s)\,y = F(s) \quad , \tag{1}$$

where y is the transversal displacement, horizontal or vertical, from the equilibrium orbit and where F(s), a quantity which describes the field errors, is given by

$$F(s) = \Delta B / B\rho \quad . \tag{2}$$

Here ΔB is a deviation from the ideal magnetic field, whereas $B\rho$ is the magnetic rigidity. It is important to keep in mind that (1) does not include the effects of nonlinearities, including those coming from the sextupoles.

PATRIS simulates the effects of imperfections by kicks, i.e. it evaluates the r.m.s. values of closed orbit deviations at various points

of interest by assuming that the right hand side of (1) is a Dirac delta[F1] function. As previously mentioned, there are four contributors to the distorted closed orbit at each point, which are considered by the code. They are:

1. Cumulative effects of the errors in the dipole integrated strength over the lattice.

2. Cumulative effects of the axial rotations of all the dipoles in the lattice.

3. Cumulative effects of the horizontal lateral displacements of all the quadrupoles in the lattice.

4. Cumulative effects of the vertical lateral displacements of all the quadrupoles in the lattice.

At each point of interest the code computes the above four entities. Each is computed under the assumption that it is the only perturber of the closed orbit and that in average the resulting r.m.s. error in the bending angle, i.e. the imperfection's kick strength, is one milliradian per magnet. Therefore, they portray the isolated influence of specific kinds of imperfections in the whole lattice on the closed orbit at a specific point of interest. The r.m.s. values are taken over 21 different distributions of random errors. These contributions are given in the columns 3 through 6 of Table 1. The last two columns of Table 1 describe the r.m.s. values of horizontal and vertical displacement at the end of each lattice element. These values are obtained by an appropriate weighting and combining of the four entities, 1 through 4, with the actual r.m.s. values of these perturbers (as opposed to those that would yield r.m.s. value of the bending angle exactly one milliradian) taken into account, and a subsequent evaluation of the r.m.s. values of closed orbit displacements over the same 21 distributions of random errors as before. Needless to say, the presence of errors breaks the periodicity of the machine, if any, and the code takes this into account by moving from one superperiod to another in such a manner that different sets of random numbers are being used in different superperiods.

As previously mentioned, Eq.(1) does not include the effects of nonlinearities in determining the closed orbit. However, one consequence of the presence of sextupoles is nevertheless handled. Namely, the distorted closed orbit does not pass through the centers of the sextupoles and, as a result, there is a feed-down effect equivalent to quadrupole gradient errors, with the subsequent tune shifts and beta variations. These are evaluated by PATRIS for each of those 21 distributions of random errors and then printed.

F1: See Appendix A for some details.

Realistic Closed Orbit Calculation and Correction

In addition to the previously described quick statistic treatment of closed orbit distortions, based on the simulation of imperfections by kicks, PATRIS is also able to handle the problem in a more realistic manner. Precise effects of the previously discussed four sources of errors are evaluated and incorporated into the 7 x 7 transfer matrix employed by PATRIS. Furthermore, nonlinearities are taken into account and simulated by kicks. The code employes one sequence of random errors per run, using different random numbers in different superperiods. This means that at the present time one has to make several runs, if a statistical treatment of the realistic closed orbit is sought. After computing the distorted closed orbit, PATRIS corrects it by using the Fermilab monitoring/correcting scheme[2,3,4].

The scheme uses a selected number of monitors and correctors which are in reality placed beside each other and which are identified with each other in the code. The beam position monitors and the sextupoles are assumed to be perfectly alligned with the reference orbit going through the quadrupole without a displacement. In addition, the beam position monitors are supposed to have ideal sensitivity. The best location for such a monitor/corrector element is the place where the relevant beta function is large. Therefore, we place all the horizontal elements beside the horizontally focusing quadrupoles, and we do the equivalent thing with the vertical monitors/correctors, i.e. we place them beside each horizontally defocusing quad. At these locations the distorted closed orbit is monitored and the corrective kicks are being delivered there, by the dipole correctors. To evaluate the strengths of the corrective kicks, the code takes the values of closed orbit displacements at three successive monitors and imposes the conditions necessary to make these displacements vanish in the absence of nonlinearities. Then the code moves one monitor forward and repeats this procedure, thereby obtaining another set of conditions. Going in this manner around the whole lattice, the code sets up a set of N equations with N unknowns, N being the number of monitor/corrector elements in the lattice. Fortunately, they can be solved by a simple successive elimination of the unknowns (see Appendix B for more details), without having to invert an N x N matrix which might be a prohibitively large task for a big lattice. In doing so, the code evaluates all the kick strengths and then reevaluates the distorted closed orbit in the presence of these corrective kicks. In the absence of nonlinearities, i.e. with the chromaticity sextupoles turned off for instance, PATRIS delivers such kicks that the residual closed orbit is zero at all the monitors, regardless of the r.m.s. values of the errors (except, of course, for grossly exaggerated values which would make the whole problem unstable). In the presence of sextupoles, however, the residual closed orbit cannot be forced to vanish exactly by this linear correcting scheme. Moreover, the presence of sextupoles aggravates the problem and the displacements of the uncorrected closed orbit get noticeably bigger with sextupoles (or other sources of nonlinearities) turned on.

This scheme, as its name indicates, has been successfully used at Fermilab and, in addition to being used in PATRIS, its versions have been incorporated also in some other tracking/analytic codes which handle the origins of closed orbit distortions in different ways.

Results of Statistic Approach to Closed Orbit Distortions in the Kick Approximation

We have made two runs over the same 21 distributions of random errors, with the cut at 2.5σ . First, we selected all four types of errors to have the same r.m.s. value 10^{-3} , in the appropriate units. However, from the subsequent realistic closed orbit analysis, it became clear that the corrected closed orbit would be prohibitively large, at this r.m.s. value of errors. Therefore, we opted for the more stringent 3×10^{-4} r.m.s. values of errors and repeated the run, keeping everything else unchanged. The results are displayed in Tables 1 and 2 and in Figures 1 through 4.

Table 1 represents the r.m.s. values of the closed orbit horizontal and vertical displacement in millimeters (the last two columns), as well as the relative importance of the four types of errors taken individually. Only one superperiod is printed, even though the code runs over all the superperiods, with the periodicity broken by random errors, in order to evaluate what is being printed for one superperiod. Two things are apparent. The r.m.s. value of closed orbit displacement follows the local size of the beta function, as one moves along the lattice. For the horizontal plane, the r.m.s. of displacement is maximum inside the horizontally focusing quad, where β_H attains its maximum, and it is minimum at the defocusing quad due to the minimum of β_H . This is even more transparent from Figures 1 and 2, where the r.m.s. values for x and y are plotted versus the magnet number in the superperiod (roughly versus the distance as one moves along the ring). We notice that the vertical plane displays a picture very similar to that of the horizontal plane except for the fact that it has been shifted by the distance between a QF and the first QD that follows. As far as the ranges are concerned, the r.m.s. value of the displacement varies between about 1.6 and 6 millimeters. Therefore, we expect that few distributions of random errors will cause the closed orbit displacements to significantly exceed 6 millimeters, even though we have been able to find two of them (out of the total of eleven that we have examined) where at one or two monitors the displacement more than doubled this value (13.5 and 13.7mm have been found). The second conclusion that can be inferred from Table 1 is that the quadrupoles have the tendency to create both the peak and average contributions bigger than those of the dipoles. When one combines this with the fact that weighting factors (in the procedure of combining the columns 3 through 6 in order to get 7 and 8) are bigger for the quadrupoles than for the dipoles, the immediate conclusion is that the quadrupole lateral displacement errors will be more important in the Booster than the errors introduced by the dipoles.A similar conclusion applies also to some other machines, the RHIC in particular.

Table 2 displays the tune shifts and the beta variations due to the effective quadrupole gradient errors, as a result of the crossing of the sextupoles by the distorted closed orbit. The beta variations are taken at the beginning of the lattice input, i.e. in the middle of a superperiod. These results are also plotted and represented in Figures 3 and 4.

Results of the Realistic Closed Orbit Calculations

As described in the Introduction, PATRIS can handle the problem of closed orbit in a more realistic and predictive manner than just simulating the lattice imperfections by kicks. However, the code in its present version performs the so-called realistic closed orbit calculations on one string of random numbers. Thus the user has the option to rely on the statistics of the kick-simulated closed orbit distortions, supplemented by a realistic closed orbit calculation for the purpose of finding the kick strengths and the residual corrected closed orbit, or, as an alternative, to run several cases of realistic closed orbit calculations for different random errors and to do statistics "by hand."

We decided to perform some statistics after getting a seemingly peculiar result, from a single realistic closed orbit run, which indicated that the vertical closed orbit displacements tend to be much bigger than the horizontal ones. The kick-simulated run over 21 distributions of random errors did not indicate such a disparity between the two planes. Nor did a realistic closed orbit calculation on the RHIC lattice indicate anything similar.

We performed calculations with 11 different sequences of random errors. Initially, we set the r.m.s. values of the four types of errors to be 10^{-3}, but this proved to be too generous. The residual corrected closed orbit, with the chromaticity sextupoles on, was in most cases still several millimeters in transverse size. Furthermore, we picked up a "bad" distribution of random errors (with the cut at 2.5σ, as mentioned) that made the maximum displacement of the corrected closed orbit to be about 13 millimeters. With sextupoles off, however, the correctors made the closed orbit exactly zero at the monitors, as expected.

Therefore, we repeated the same 11 runs, but this time with the r.m.s. values of the four types of errors reduced to 3×10^{-4}, in the appropriate units. In all of these 11 cases, the corrected closed orbit this time fell within one millimeter. We have also tested how the corrected closed orbit gets worse with an increase of the r.m.s. values of the four kinds of errors, on the worst distribution of random errors that we had encountered. While even this comparatively rather bad distribution yielded a corrected closed orbit that fell within one millimeter for the 3×10^{-4} errors, it reached 1.36 mm at one location for the 4×10^{-4} errors and it barely passed 2 millimeters at four (out of 48) monitors for the 5×10^{-4} errors.

These facts have given us the necessary confidence to claim that if a 3×10^{-4} level of r.m.s. values is attained in the real machine, the Fermilab correcting scheme alone will be able to successfully handle the closed orbit distortions arising from the four types of errors we have discussed. The results of the run over the worst distribution of random errors are shown in Table 3. They deviate quite appreciably from the r.m.s. values of displacements at the same monitors given in Table 1. However, we emphasize

that this is a bad case and that most other cases display displacements whose sizes are much closer to the averaged predictions over 21 cases. The results from Table 3 are also plotted in Figures 5 and 6. These figures represent the uncorrected and corrected closed orbit for the two planes. The reader will undoubtedly notice that the uncorrected closed orbit behaves in the horizontal plane much worse than in the vertical one. This is obviously a consequence of the particular set of random errors. We have inspected the results of all of the eleven runs and have found the closed orbit distortions bigger in the horizontal plane in four cases. It was just the opposite in another group of four cases, whereas in the remaining three runs the distortions were about equal in the two planes.

Conclusion

In this note, we have handled four major sources of closed orbit distortions: errors in the dipole integrated field strength $\Delta(Bl)/Bl$, axial rotation of the dipole, and the two possible lateral displacements of the quadrupole. This list is by no means exhaustive. Some other major errors that we have not addressed so far are errors due to the axial rotation of the quadrupole, errors in the field gradient strength $\Delta K/K$ for the quadrupole, and various higher order multipoles present both in the dipole and in the quadrupole. We are currently working on some of these issues and we also plan to address some others in the future.

As far as the four types of errors that we have discussed are concerned, our conclusion is clear: one should strive to achieve the 3×10^{-4} level of r.m.s. values and this is very likely sufficient for the Fermilab correcting scheme to work well. We definitely support the implementation of this scheme on the Booster. Its implementation will require installing a beam position monitor, followed by a dipole corrector, beside each quadrupole. The maximum integrated field strength for such a bump corrector, to be able to correct the orbit at the top magnetic rigidity of 18 Tm, is predicted to be about 55 Gauss*meters. This estimation may have to be somewhat changed in the future, once other sources of errors are brought in for an analysis. But the essentials of the correcting scheme should remain unchanged.

However, there is an unpleasant scenario that cannot be completely ruled out. If, by some unfortunate circumstances, on Day 1 we find a very bad orbit, we will have to rely on other means, like physically moving quads and Fourier harmonic compensation, to bring first the errors down to the levels at which the proposed local correction scheme will work.

Appendix A

Here we give the reader a basic idea on how PATRIS handles closed orbit errors in the kick approximations. The closed orbit deviation y_i at the i-th location, where $\beta = \beta_i$ and the phase advance is ϕ_i, is given by

$$y_i = \frac{1}{2\sin(\pi\nu)} \sum_{j>i} \sqrt{\beta_i \beta_j}\ \theta_j \cos\nu(\pi + \phi_i - \phi_j) \quad , \qquad (A.1)$$

where the summation is over all the errors of strength θ_j (in equivalent kick-angle) at the location with $\beta = \beta_j$ and phase advance $\phi_j > \phi_i$. This formula for y_i is used by PATRIS, which also takes care of the proper ordering of the phase advances (i.e. $\phi_j > \phi_i$). The expression (A.1) can easily be derived by starting from the periodic solution to the equation of motion (Eq. 1 in the main body of this note) rewritten in Floquet coordinates (Eq. (4.6) of Ref. 1) and inserting the appropriate sum of Dirac delta functions as the perturber $f(\psi)$ in Eq. (4.7) of Ref. 1.

Summation in (A.1) is linear and the two degrees of freedom are decoupled

$$y_i^H = \sum_{\text{DIPOLE/H}} + \sum_{\text{QUAD/H}} = y_i^{H,D} + y_i^{H,Q} \qquad (A.2)$$

$$y_i^V = \sum_{\text{DIPOLE/V}} + \sum_{\text{QUAD/V}} = y_i^{V,D} + y_i^{V,Q} \qquad (A.3)$$

The code first computes each of the above four sums individually, assuming that <u>at each magnet</u>

$$(\theta_j)_{\text{r.m.s.}} = 1 \text{ mrad} \qquad (A.4)$$

Once the four quantities $y_i^{H,D}$, $y_i^{H,Q}$, $y_i^{V,D}$, $y_i^{V,Q}$ are found for each of 21 distributions of random numbers, the r.m.s. values of these four quantities are evaluated. They describe partial contributions to the total closed orbit distortion, where "partial contribution" means that it is evaluated under the assumption that it is the only present perturber. Since these

quantities are evaluated under the assumption that (A.4) is true at each magnet, they describe the relative importances of various sources of errors.

In order to find the r.m.s. values of the distorted closed orbit displacements, under the r.m.s. error values specified on the input by the user, PATRIS first abandons (A.4) and replaces $(\Theta_j)_{r.m.s.}$ by the actual r.m.s. values it computes on the basis of the input given r.m.s. values for the errors. Then it evaluates the four sums on the basis of these actual r.m.s. values for Θ_j, adds them up to get (A.2) and (A.3) and then takes the r.m.s. values for y_i^H and y_i^V, over the 21 distributions of random numbers.

Appendix B

In this appendix we sketch the basic principles of the so-called three bump method used in the Fermilab monitoring/correcting scheme. As described in the main text of this note, a certain number of monitors and correctors are placed at preferred locations, i.e. beside the quadrupoles where the relevant beta function is large. It is assumed that the monitors have ideal sensitivity and that they are perfectly alligned with the reference orbit going through the quadrupole without a displacement.

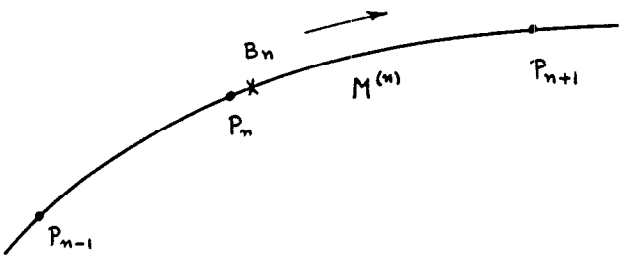

The above drawing displays the particle trajectory through the three points of interest. Consider what is happening at the n-th beam position monitor and its two immediate neighbors. We label the monitor/corrector block by P_n and the phase space point at P_n by X_n, i.e. X_n will be the following column vector

$$X_n = \begin{pmatrix} y \\ y' \\ 1 \end{pmatrix}_{At\ P_n} = \begin{pmatrix} y_n \\ y'_n \\ 1 \end{pmatrix} \tag{B.1}$$

We also know the transfer matrix in the absence of errors between any pair of monitors (it is part of the full 7 x 7 transfer matrix between the two monitors in PATRIS). Let $M^{(n)}$ label the transfer matrix between the monitors P_n and P_{n+1}. For one transverse degree of freedom its form is

$$M^{(n)} = \begin{pmatrix} m_{11}^{(n)} & m_{12}^{(n)} & 0 \\ m_{21}^{(n)} & m_{22}^{(n)} & 0 \\ 0 & 0 & 1 \end{pmatrix} \tag{B.2}$$

with the symplectic condition $\det M^{(n)} = 1$ being fulfilled

$$m_{11}^{(n)} m_{22}^{(n)} - m_{12}^{(n)} m_{21}^{(n)} = 1 \qquad (B.3)$$

Suppose that the correctors deliver kicks with the kick angle Θ_n at the n-th monitor/corrector P_n. The effect of such a kick is described by the following matrix

$$B_n = \begin{pmatrix} 1 & 0 & 0 \\ 0 & 1 & \Theta_n \\ 0 & 0 & 1 \end{pmatrix} \qquad (B.4)$$

Let these kicks be such that they steer the on-momentum particle trajectory precisely through the positions X_n (in the absence of errors). Then the condition

$$X_{n+1} = M^{(n)} B_n X_n \qquad (B.5)$$

must be fulfilled. Written out in components (B.5) is just

$$y_{n+1} = m_{11}^{(n)} y_n + m_{12}^{(n)} y_n' + m_{12}^{(n)} \Theta_n \qquad (B.6a)$$

$$y_{n+1}' = m_{21}^{(n)} y_n + m_{22}^{(n)} y_n' + m_{22}^{(n)} \Theta_n \qquad (B.6b)$$

We solve (B.6a) for y_n'

$$y_n' = \frac{y_{n+1} - m_{11}^{(n)} y_n - m_{12}^{(n)} \Theta_n}{m_{12}^{(n)}} \qquad (B.7)$$

and increment the label by 1 to obtain

$$y_{n+1}' = \frac{y_{n+2} - m_{11}^{(n+1)} y_{n+1} - m_{12}^{(n+1)} \Theta_{n+1}}{m_{12}^{(n+1)}} \qquad (B.8)$$

Now insert y_n' from (B.7) into (B.6b) and equate the resulting y_{n+1}' with (B.8)

$$\frac{y_{n+2} - m_{11}^{(n+1)} y_{n+1} - m_{12}^{(n+1)} \theta_{n+1}}{m_{12}^{(n+1)}} =$$

$$m_{21}^{(n)} y_n + m_{22}^{(n)} \theta_n + m_{22}^{(n)} \left(\frac{y_{n+1} - m_{11}^{(n)} y_n - m_{12}^{(n)} \theta_n}{m_{12}^{(n)}} \right) =$$

$$m_{21}^{(n)} y_n - \frac{m_{22}^{(n)} m_{11}^{(n)}}{m_{12}^{(n)}} y_n + \frac{m_{22}^{(n)}}{m_{12}^{(n)}} y_{n+1} = - \frac{y_n}{m_{12}^{(n)}} + \frac{m_{22}^{(n)}}{m_{12}^{(n)}} y_{n+1} \quad , \qquad (B.9)$$

where (B.3) has been used to simplify the expression on the right hand side of the above equation. This equation can now be solved for θ_{n+1} , i.e.

$$\theta_{n+1} = \frac{y_{n+2} - m_{11}^{(n+1)} y_{n+1}}{m_{12}^{(n+1)}} + \frac{y_n}{m_{12}^{(n)}} - \frac{m_{22}^{(n)}}{m_{12}^{(n)}} y_{n+1} \qquad (B.10)$$

By decrementing the index n by one unit we get

$$\theta_n = \frac{y_{n-1}}{m_{12}^{(n-1)}} - \left(\frac{m_{11}^{(n)}}{m_{12}^{(n)}} + \frac{m_{22}^{(n-1)}}{m_{12}^{(n-1)}} \right) y_n + \frac{y_{n+1}}{m_{12}^{(n)}} \qquad (B.11)$$

Therefore, the kick angle θ_n at the n-th bump corrector is completely determined by the displacements at the n-th monitor and at its two immediate neighbors, i.e. at the (n-1)-th and (n+1)th locations.

In the absence of corrective kicks, the n-th beam position monitor P_n will read the closed orbit displacement r_n at the n-th location, the displacement being nonzero due to the presence of errors. To compensate for the effects of errors, one simply sets $y_n = - r_n$ and evaluates the necessary kick angle θ_n to create a reverse displacement in the absence of errors. In the presence of errors and with sextupoles off, these kicks will precisely cancel the actual displacement at the beam position monitors. With sextupoles on, however, a precise cancelation does not occur, but the residual displacements are to a significant degree reduced.

References

1. E. Courant & H. Snyder, Annals of Physics 3, 1 (1958).

2. R. Raja, A. Russell & C. Ankenbrandt, Nucl. Inst. & Meth. A242, 15 (1985)

3. A. G. Ruggiero, Some Calculations for TRISTAN

4. B. Autin, Lattice Perturbations, AIP Conference Proceedings, No 127, p. 139

Tables

1. This table represents the output from PATRIS for the kick-modeled statistical handling of closed orbit distortions. The statistics is taken over 21 distributions of random errors, with the r.m.s. values of all errors 3×10^{-4}, in the appropriate units. The random number sequences were cut at 2.5σ.

2. This table represents the tune shifts and beta variations due to the crossing of the sextupoles by the distorted closed orbit, for the same run as the run presented in Table 1. The 21 rows in the table correspond to the 21 distributions of random errors.

3. This table represents the output from PATRIS for the realistic closed orbit calculation over the worst distribution of random errors. Note that the corrected closed orbit falls within one millimeter. Also note that the code supplies the correctors' kick strengths.

Table 1

CPU-TIME SO FAR = 907 MSEC
CPU-TIME SO FAR = 907 MSEC
CPU-TIME SO FAR = 907 MSEC

KW(12) = 1

CLOSED ORBIT ANALYSIS

QX = 4.81999 QY = 4.83000

LOCAL RMS EXPECT. VALUES OF CLOSED ORBIT DISPLACEMENT FOR FIELD AND MISALLIGNMENT ERRORS
CORRESPONDING TO AN RMS ERROR IN BENDING ANGLE OF ONE MILLIRAD
UNITS ARE IN MILLIMETERS

J	MAGNET	DIPOLE/H	DIPOLE/V	QUAD/H	QUAD/V	DH	DV
1	SYM	34.1424	62.4629	51.5474	108.2065	2.3860	4.9726
2	QD	46.9268	91.2395	46.7556	87.4296	2.5047	4.6139
3	MD/2	41.8943	86.6139	50.8083	114.2536	2.3411	4.9893
4	MD/2	32.3558	67.5670	41.9168	86.7636	1.8144	4.0977
5	QD	51.1750	93.6763	43.5352	78.8393	2.0566	4.0720
6	PV	40.2450	76.5396	44.6229	87.9374	2.2125	4.2045
7	DRS	44.9617	85.9459	35.9148	48.5022	1.8396	2.9752
8	MB1	36.9969	68.9437	40.7543	82.6699	1.9356	3.5978
9	SCE	37.5170	64.3382	49.5880	92.1082	2.3405	4.3978
10	B/2	50.1177	66.3646	64.4793	109.1401	3.3006	5.3139
11	MBM	56.8736	62.2042	69.7308	86.3111	2.9365	3.8248
12	SCM	51.9800	59.9435	63.4584	70.9424	3.2479	4.1055
13	SCM	50.0880	63.3688	56.9722	70.4031	2.9756	3.4148
14	MBM	41.3867	44.4141	57.0276	65.5120	2.7167	3.0226
15	B/2	44.6737	46.1767	69.7711	63.6573	3.1078	2.7646
16	SCE	63.7565	47.6963	81.8566	65.8150	4.0974	3.1850
17	MB2	80.8778	58.4909	86.6561	58.5421	3.3923	2.4614
18	DRL	54.6260	35.3032	97.6845	61.0057	4.4147	2.8095
19	QF	78.2169	41.7238	70.6985	44.8769	3.2038	2.0488
20	MF/2	70.2516	36.6092	80.0928	46.9606	4.0698	2.3683
21	MF/2	74.1443	41.9767	105.7875	51.9187	5.0330	2.5106
22	QF	66.6987	35.9419	67.6093	42.9167	2.8955	1.6541
23	PH	45.4297	25.4464	84.5142	43.7450	3.8657	1.8950
24	DRS	57.5008	36.3375	73.2533	35.4344	3.5035	1.8220
25	DRE	60.3898	53.2137	77.2260	72.2046	3.5822	3.3750
26	DRL	44.3105	72.0866	58.3781	99.4180	3.0471	5.3758
27	QD	29.6556	54.8973	38.2330	83.8856	1.8305	4.2428
28	MD/2	37.7447	76.9121	57.0717	102.2162	2.4885	4.1582
29	MD/2	38.3530	71.1645	39.8767	74.9363	2.0269	3.6281
30	QD	33.8295	68.8945	53.1300	121.5205	2.2895	5.2036
31	PV	42.3166	75.2917	66.5302	116.9762	2.6822	4.8038
32	DRS	48.1931	91.4539	55.3550	106.1555	2.9175	5.4518
33	MB1	31.4976	59.3912	48.2243	91.9727	2.3598	4.4750
34	SCE	36.0760	62.4300	48.2906	100.9824	2.5870	4.9731
35	B/2	41.9839	58.0348	45.3420	83.8060	2.2081	3.6120
36	MBM	53.7601	64.5687	57.3234	67.2014	3.2288	3.9282
37	SCM	55.8515	62.9074	48.1207	55.8173	2.3138	2.2937
38	SCM	48.4571	55.7270	75.8144	80.6698	3.4994	3.4976
39	MBM	57.2378	60.7091	77.2625	75.1771	3.2436	2.9840
40	B/2	43.3665	46.8508	79.0596	69.6823	3.6861	3.3114
41	SCE	66.0963	53.9649	79.7879	61.5983	3.6091	2.9191
42	MB2	76.3312	60.0233	98.8875	78.2977	4.4009	3.2498
43	DRM	66.2877	44.9891	111.0294	69.6991	4.7105	2.9244

(continues on the next page)

Table 1 (continued from the previous page)

44	SF	65.5889	44.1038	105.8447	75.5161	4.0710	2.8740
45	DRS	63.8717	33.7138	108.7015	62.4363	4.7410	2.6460
46	QF	73.0857	40.8793	91.8641	56.1604	4.7758	2.8141
47	MF/2	77.5508	44.8610	104.5140	58.6718	4.6618	2.7106
48	MF/2	76.1759	41.9782	101.6964	63.9993	4.9026	2.9551
49	QF	67.2282	37.5805	69.6501	58.7996	2.8512	2.4192
50	PH	47.9311	25.9317	109.0874	61.7991	4.8593	2.7560
51	DRS	66.7795	38.6400	114.1038	61.0388	5.7994	2.9306
52	MB1	61.2078	40.1776	79.0207	48.6922	3.4544	2.1577
53	SCE	71.8025	46.9227	112.8430	62.4180	4.5820	2.5437
54	B/2	56.2526	42.7402	65.8480	56.8849	3.0140	2.6744
55	MBM	57.3593	50.6525	90.0438	76.6670	4.5147	3.8265
56	SCM	72.4169	69.0431	59.7913	52.2838	2.5771	2.4529
57	SCM	60.1945	55.7484	85.5428	70.3801	3.4457	2.5922
58	MBM	60.1863	49.9912	69.2573	75.8769	3.3581	3.5730
59	B/2	51.0820	59.4923	68.3608	68.0105	3.2771	3.4562
60	SCE	45.3781	75.0903	68.4798	109.5217	2.7688	5.0174
61	MB2	50.3401	63.5964	63.2003	95.5318	2.6132	4.1598
62	DRL	36.3770	56.3187	63.7930	102.3806	2.7806	3.9993
63	QD	50.0845	97.0447	37.0067	85.4531	1.5697	3.6361
64	MD/2	34.2016	70.7855	62.2052	86.4740	2.9675	4.4966
65	MD/2	40.1811	90.3401	46.2989	92.7989	2.1236	4.5656
66	QD	36.7371	69.1103	52.7782	105.3233	2.6194	5.1519
67	PV	26.3244	52.1597	51.6527	107.5784	2.3310	4.5653
68	DRS	51.4825	97.6242	43.2960	83.2966	2.4018	4.4253
69	MB1	44.5465	80.6160	48.6971	94.0857	2.5859	4.4454
70	SCE	40.5456	73.1297	55.7242	82.9114	2.8039	4.5531
71	B/2	47.8535	73.9917	57.0529	99.0409	2.2832	4.2853
72	MBM	45.7084	57.7206	64.6181	75.0749	2.8808	3.4091
73	SCM	49.9811	62.0832	66.3641	81.1582	2.5546	3.5519
74	SCM	47.3958	52.8367	45.6483	62.3038	2.7504	3.5311
75	MBM	68.8657	75.7482	61.6991	93.2868	3.4209	4.5831
76	B/2	56.8592	55.7870	69.9642	62.1394	3.2643	3.5402
77	SCE	70.9187	58.2704	83.8175	58.0223	4.3747	3.2140
78	MB2	61.7509	47.1505	83.6733	68.6233	4.3238	3.3696
79	DRM	52.9491	38.8470	87.9912	55.7328	4.1591	2.8038
80	SF	72.3445	50.9974	98.5635	57.8417	4.5519	2.7261
81	DRS	84.7067	54.3639	93.2784	57.7541	5.0341	3.3677
82	QF	66.5069	37.0333	92.7497	48.3071	4.4405	2.3900
83	MF/2	84.9647	47.4913	99.3969	50.9040	5.2785	2.7564
84	MF/2	72.2581	39.9690	90.3620	54.8076	4.0223	2.5462
85	QF	74.9281	40.0352	90.5227	56.0333	4.6970	2.9412
86	PH	66.2925	36.0664	83.7602	44.8437	4.2598	2.2945
87	DRS	49.3348	29.1435	68.8260	46.4618	2.9674	2.0333
88	MB1	64.2451	43.6293	79.4980	60.7411	3.5669	2.5546
89	SCE	62.1525	37.7192	80.8476	45.6976	3.4369	1.9040
90	B/2	63.4346	39.0929	71.2342	61.7065	3.0788	2.7091
91	MBM	55.8752	56.8933	80.3579	78.1341	3.5623	3.6218
92	SCM	49.5924	47.6881	62.4535	70.3354	3.2075	3.6429
93	SCM	55.8625	57.7513	81.3244	74.8291	3.4681	3.3370
94	MBM	43.3712	39.0250	67.0749	62.2060	2.9423	2.7398
95	B/2	50.1054	53.8483	53.9725	57.4023	2.5137	2.6607
96	SCE	33.6299	50.3371	57.1199	62.5416	2.6265	3.1274
97	MB2	42.8946	56.9038	54.3770	85.3369	2.3888	3.5531
98	DRM	42.8988	73.0687	43.3213	91.4408	2.4381	4.8948
99	SD	39.9989	72.3284	51.7663	88.8019	2.1226	3.5340
100	DRS	43.9229	87.6509	64.1925	97.5296	2.7794	4.0768
101	QD	51.4992	103.1485	57.0354	118.6530	2.9068	6.0751
102	MD/2	38.8774	78.6138	53.1053	92.8431	2.1611	3.8172
103	MD/2	36.1014	70.0006	44.4112	68.6998	1.9816	3.4507

(continues on the next page)

Table 1 (continued from the previous page)

104	QD	35.9044	67.7901	58.6541	113.5617	2.8959	5.4924
105	PV	47.9916	91.4890	58.2640	102.6689	2.5354	4.5804
106	DRS	52.2747	105.7921	45.8753	98.7989	2.3631	5.1395
107	DRE	56.3082	65.9248	54.8539	65.2737	2.6618	3.2141
108	DRL	67.4115	43.6141	79.3874	45.1759	4.2827	2.3151
109	QF	59.8051	32.9614	82.1359	42.7979	3.8251	1.8757
110	MF/2	78.0115	43.2899	99.2966	49.2989	4.6892	2.3847
111	MF/2	74.2679	38.4028	68.4186	47.5451	3.6398	2.0114
112	QF	78.8503	42.1145	86.6037	44.7321	4.9226	2.4458
113	PH	65.3096	38.5779	93.0102	45.6027	3.9759	2.0100
114	DRS	57.4235	34.2591	129.5847	66.5277	5.8268	3.0503
115	MB1	76.4914	45.4747	96.7656	59.7384	5.0596	3.1272
116	SCE	79.0885	49.0645	78.4361	61.5689	3.7646	3.0277
117	B/2	86.3912	59.3602	97.9627	73.1751	4.3487	3.4162
118	MBM	50.0189	50.7425	88.8913	73.1722	3.4291	2.9234
119	SCM	57.0827	52.2904	60.8297	53.5524	2.6674	2.5331
120	SCM	58.5348	52.9670	81.6829	50.0935	4.1727	2.9688
121	MBM	67.3293	57.6061	79.1585	71.9281	4.2442	3.5407
122	B/2	44.3541	48.8346	60.0689	62.1500	3.1358	3.2094
123	SCE	50.3471	63.5645	52.1395	97.2736	2.5850	4.0620
124	MB2	53.7508	62.5285	66.5265	70.3480	2.9210	2.8607
125	DRM	51.0840	71.2259	46.3856	70.8895	2.3480	3.5937
126	SD	43.1409	76.6877	56.9336	100.9635	2.8639	4.8726
127	DRS	41.4856	81.5199	44.7795	89.3885	2.3618	4.5734
128	SYM	40.5074	82.5170	50.9792	94.9931	2.6314	4.8764

CPU-TIME SO FAR = 13050 MSEC
CPU-TIME SO FAR = 13050 MSEC

1

Table 2

CLOSED ORBIT ANALYSIS WITH SEXTUPOLES

TUNE SHIFTS AND BETA VARIATIONS

	HORIZONTAL		VERTICAL	
	DBETA/BETA	D-TUNE	DBETA/BETA	D-TUNE
1	0.35986e-02	0.67646e-04	0.20248e-02	0.55865e-04
2	0.87661e-02	0.28109e-02	-0.36719e-02	0.31661e-03
3	-0.34446e-02	0.13982e-02	0.12921e-01	-0.12674e-02
4	-0.51444e-02	-0.30722e-02	0.10382e-01	0.32857e-02
5	0.34473e-02	0.23414e-03	-0.10523e-01	0.82913e-03
6	0.83141e-02	0.15707e-02	-0.84879e-02	0.79469e-03
7	-0.54302e-02	0.28144e-04	0.63170e-02	0.19825e-02
8	0.17500e-01	0.69144e-02	-0.68454e-02	-0.15292e-02
9	-0.20588e-02	0.56023e-03	0.70723e-02	-0.14308e-02
10	-0.56593e-02	-0.33207e-02	-0.76399e-02	0.34624e-02
11	-0.25092e-02	-0.12864e-02	-0.46559e-02	0.58659e-03
12	0.96144e-02	0.13351e-02	-0.28951e-02	0.17469e-02
13	0.11041e-01	0.52351e-02	-0.24901e-02	-0.23369e-02
14	-0.16015e-03	-0.17859e-02	-0.65663e-02	0.36037e-02
15	-0.57906e-02	-0.40243e-04	0.59524e-02	-0.57185e-03
16	-0.42458e-03	-0.18543e-03	0.42070e-02	0.16501e-02
17	-0.87577e-02	-0.47354e-02	-0.84466e-02	0.15660e-02
18	0.14788e-02	-0.15164e-02	-0.71469e-03	0.29325e-02
19	0.17838e-01	0.78069e-02	-0.12690e-01	-0.30189e-02
20	-0.19558e-02	-0.40741e-03	-0.10504e-03	-0.10229e-03
21	0.60399e-02	0.25056e-02	-0.31512e-02	-0.18314e-02
r.m.s. values:	0.79777e-02	0.32183e-02	0.72304e-02	0.20317e-02

CPU-TI

END OF THE RUN PATRIS VRSN 3.2

Table 3

CLOSED ORBIT CALCULATION
HORIZ. AND VERT. BEAM POSITION IN MILLIMETERS
CORRECTION KICKS IN MILLIRADIANS

J	UNCORRECTED HORIZONTAL	UNCORRECTED VERTICAL	KICK	CORRECTED HORIZONTAL	CORRECTED VERTICAL
6		-0.92194	0.18111		-0.45939
23	10.12012		0.03835	0.10218	
31		3.88861	-0.03599		-0.31554
50	9.57186		0.28239	-0.66390	
67		3.71855	-0.07223		0.18869
86	-8.05008		-0.05798	-0.13719	
105		-0.73995	-0.03598		0.41233
113	-13.70112		0.01557	0.70296	
134		-3.71346	0.08472		0.10853
151	-0.84471		-0.00749	0.50068	
159		-2.56222	0.19851		-0.22432
178	13.41798		0.07847	-0.36154	
195		-0.32193	0.09358		-0.19626
214	7.45959		0.00510	-0.10076	
233		1.19418	0.07701		0.12930
241	-9.40379		-0.28294	0.54615	
262		0.07605	-0.02518		0.27382
279	-9.70533		-0.03315	0.37810	
287		-0.83249	-0.11790		0.03075
306	3.52202		0.16959	-0.34181	
323		0.90092	0.07491		-0.25459
342	9.48160		0.02158	-0.51836	
361		0.43608	-0.02291		-0.19744
369	1.64723		0.06746	0.33447	
390		-0.35055	0.25011		0.13852
407	-9.10793		-0.01462	0.69643	
415		-3.78490	-0.03850		0.28323
434	-7.51194		-0.08794	0.13273	
451		-1.44904	-0.05165		-0.01733
470	5.82112		0.01812	-0.40363	
489		3.55890	0.03819		-0.32491
497	10.80783		0.00256	-0.30167	
518		3.11626	0.14751		-0.07292
535	1.00263		-0.03338	0.17267	
543		-3.52998	0.13426		0.37629
562	-9.87146		-0.08172	0.42535	
579		-6.92929	0.11592		0.19539
598	-5.56859		-0.00874	0.34849	
617		-2.10298	0.08569		-0.39199
625	6.93407		0.05039	-0.13672	
646		4.58607	0.13266		-0.46068
663	9.17284		0.15280	-0.43833	
671		3.20464	0.03185		0.24745
690	-2.86547		-0.01527	-0.16036	
707		-3.05295	0.13318		0.61314
726	-10.48586		0.01124	0.38018	

Figure Captions

1. This figure represents the r.m.s. values of the closed orbit horizontal displacement at the end of each magnet, as given in Table 1.

2. This figure represents the r.m.s. values of the closed orbit vertical displacement at the end of each magnet, as given in Table 1.

3. This figure represents the plot of the tune shifts due to the crossing of the sextupoles by the distorted closed orbit. The 21 points in the diagram correspond to the 21 different random error distributions.

4. This figure represents the plot of the beta variations due to the same reason as the tune shifts represented in Figure 3.

5. This figure represents the plot of the closed orbit horizontal displacement at each horizontal monitor/corrector element. The results are those obtained from the "worst" encountered random error distribution in the set of realistic closed orbit calculations. The term "worst" here means to describe the case of the biggest displacements in either of the two planes, seen in the group of 11 runs. The plot also includes the corrected closed orbit.

6. This figure represents the results of the same run, with the same "worst" distribution of errors,as in Figure 5, but for the vertical plane.

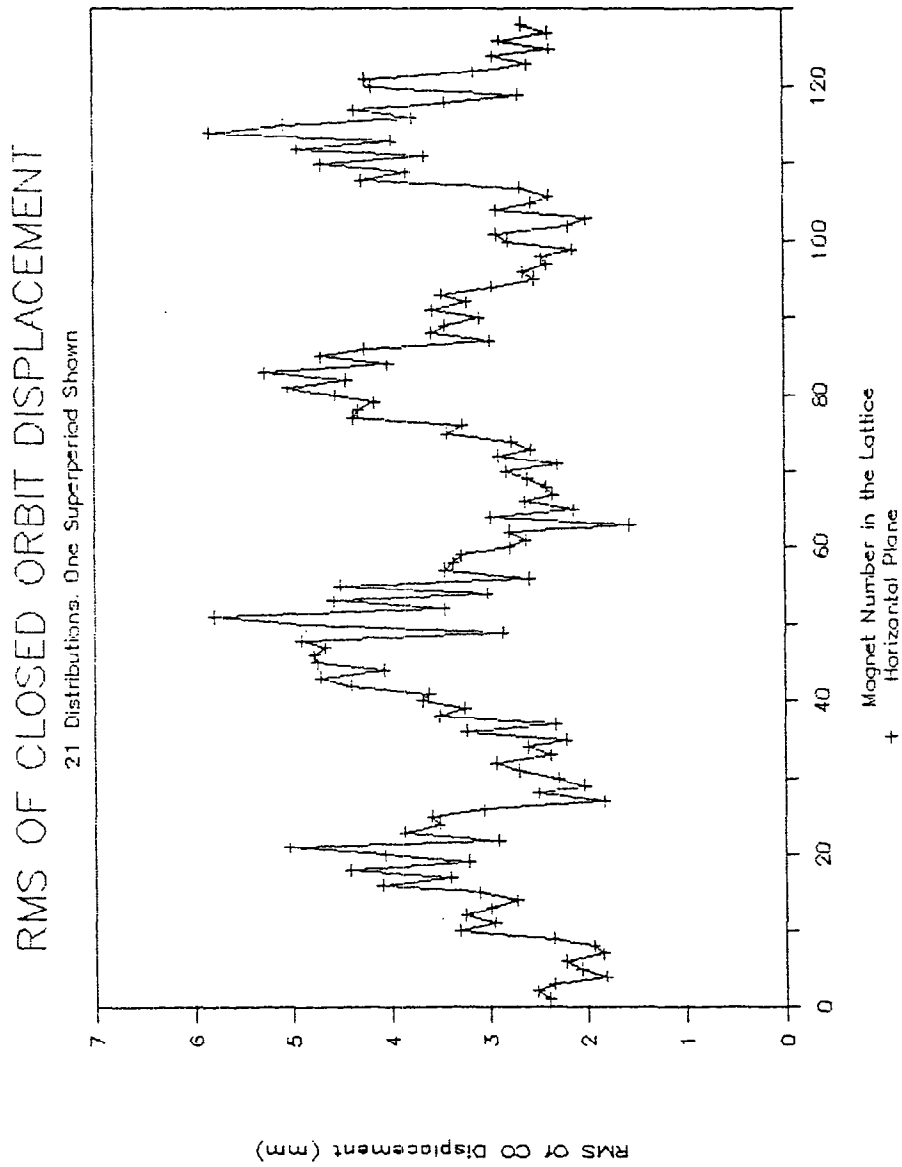
RMS OF CLOSED ORBIT DISPLACEMENT
21 Distributions, One Superperiod Shown
RMS σ & Displacement (mm)
0
1
2
3
4
5
6
7
0
20
40
60
80
100
120
Magnet Number in the Lattice
+ Horizontal Plane

Figure 1

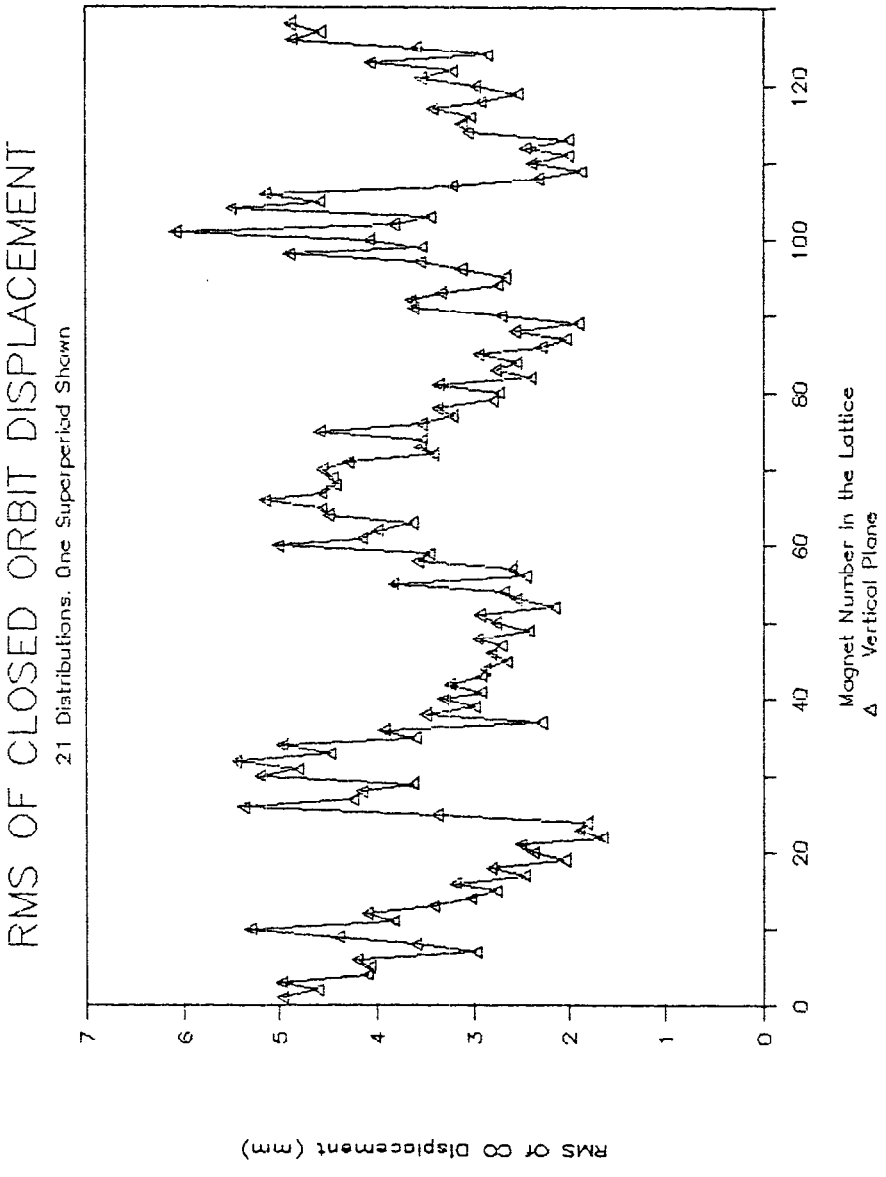
RMS OF CLOSED ORBIT DISPLACEMENT
21 Distributions, One Superperiod Shown
RMS of 8 Displacement (mm)
0
1
2
3
4
5
6
7
0
20
40
60
80
100
120
Magnet Number in the Lattice
Δ Vertical Plane

Figure 2

Figure 3

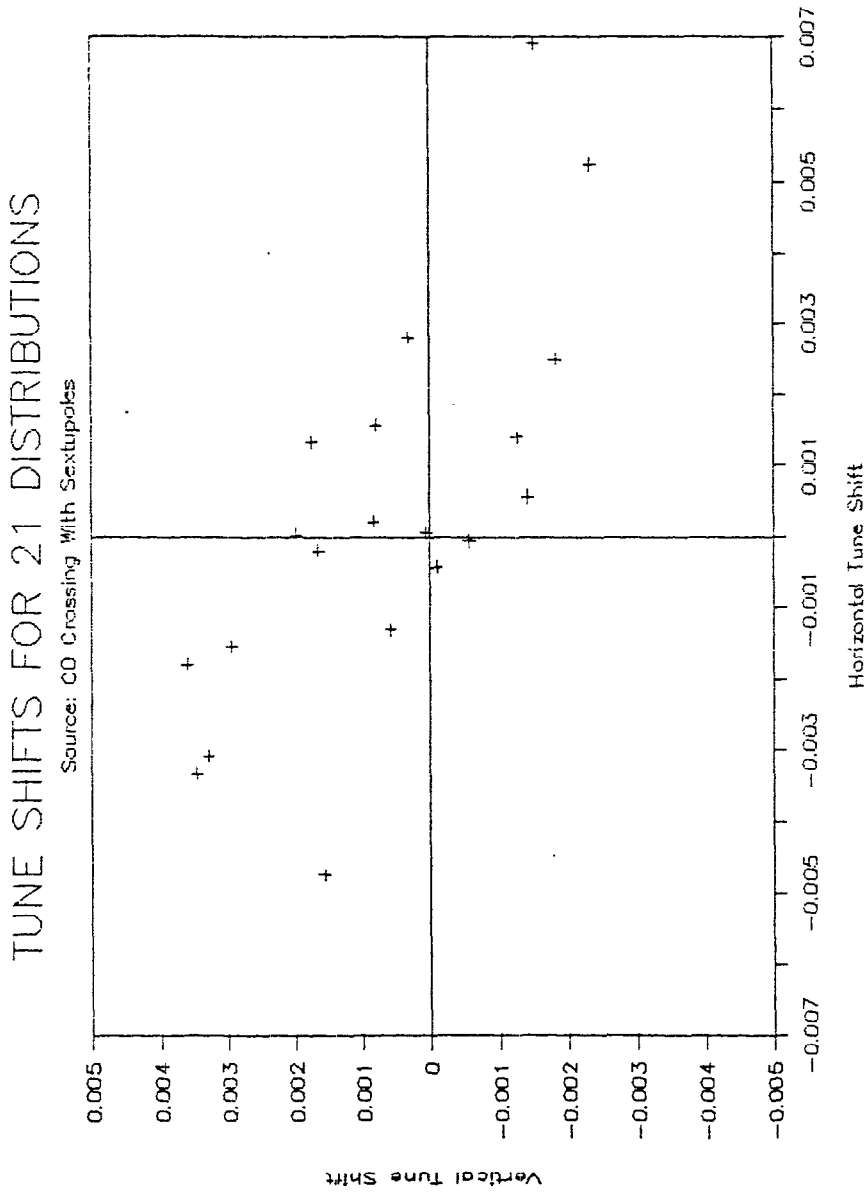
TUNE SHIFTS FOR 21 DISTRIBUTIONS
Source: CO Crossing With Sextupoles
Vertical Tune Shift
Horizontal Tune Shift
0.005
0.004
0.003
0.002
0.001
0
-0.001
-0.002
-0.003
-0.004
-0.005
-0.007
-0.005
-0.003
-0.001
0.001
0.003
0.005
0.007

Figure 4

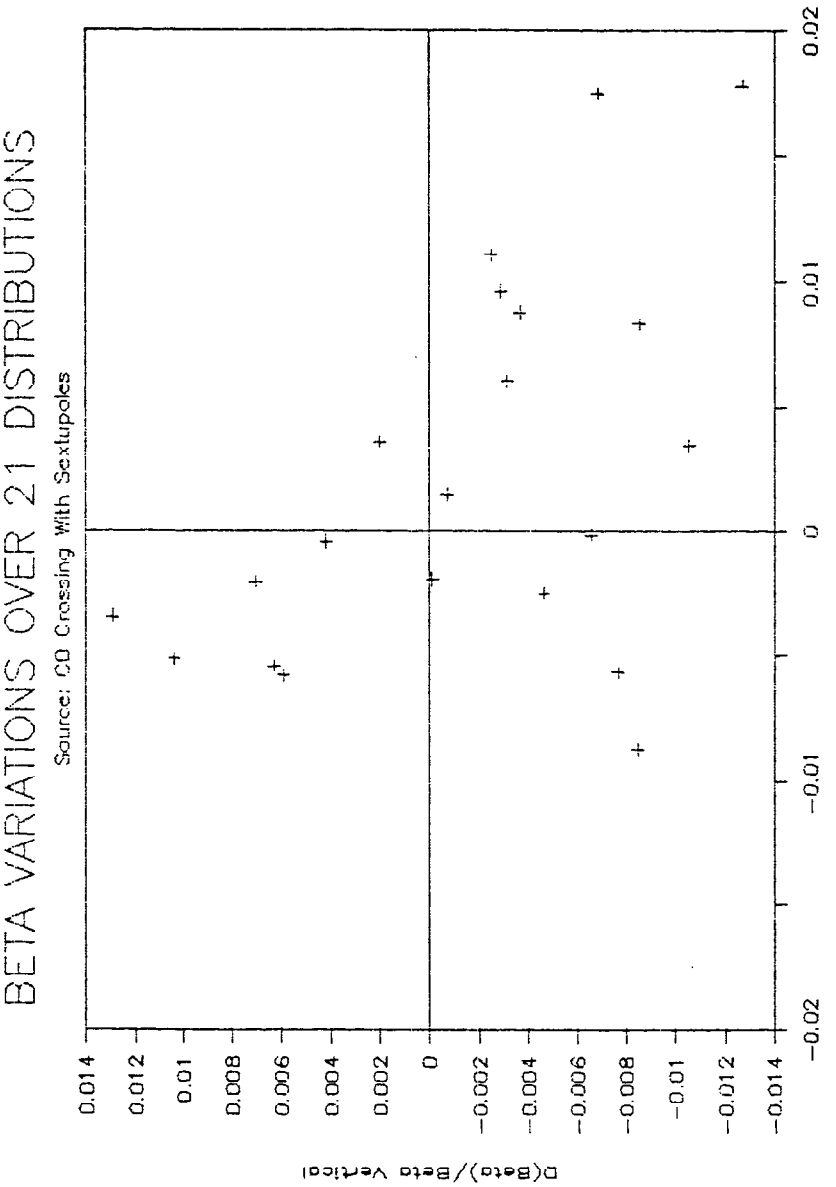
BETA VARIATIONS OVER 21 DISTRIBUTIONS
Source: CO Crossing With Sextupoles
D(Beta)/Beta Vertical
0.014
0.012
0.01
0.008
0.006
0.004
0.002
0
−0.002
−0.004
−0.006
−0.008
−0.01
−0.012
−0.014
−0.02
−0.01
0
0.01
0.02
D(Beta)/Beta Horizontal
+ Mid. of Superperiod

Figure 5

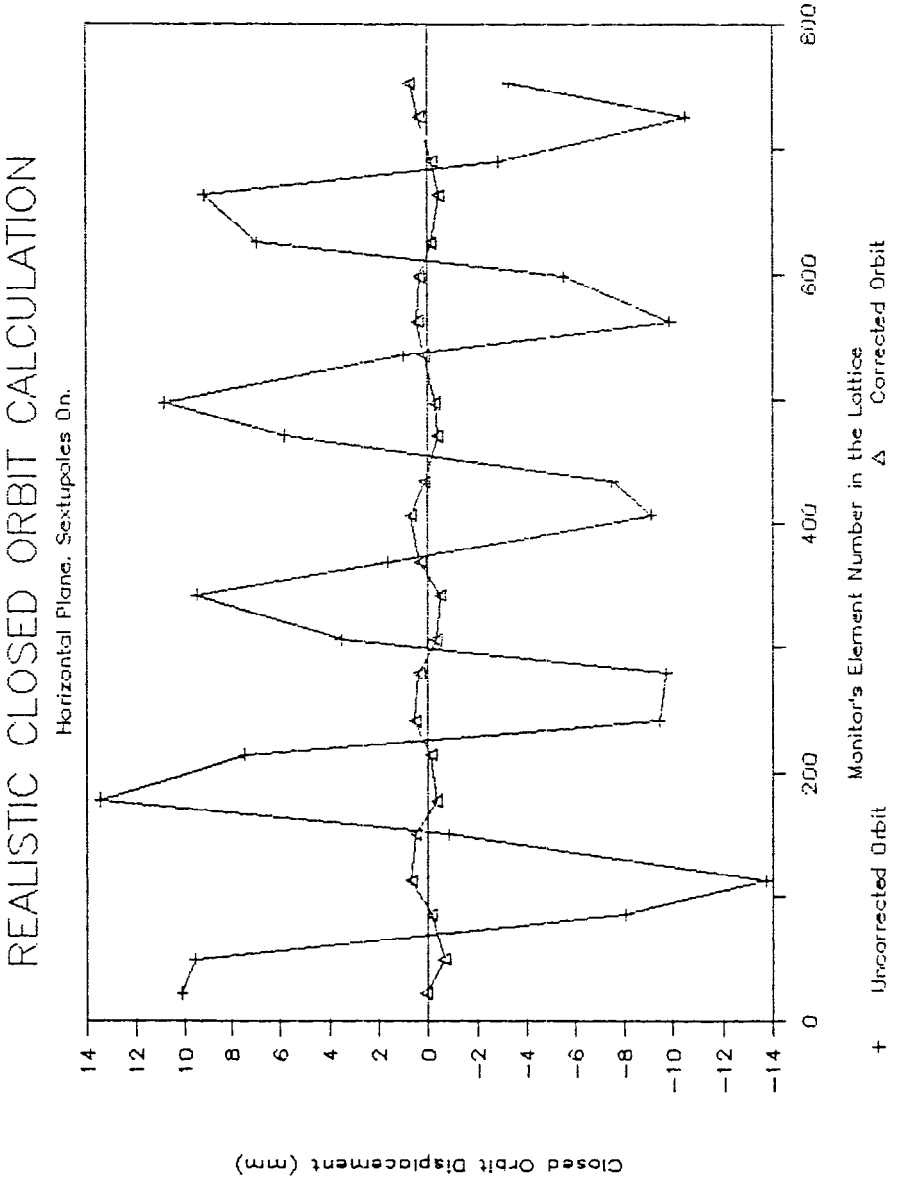
REALISTIC CLOSED ORBIT CALCULATION
Horizontal Plane, Sextupoles On.
Closed Orbit Displacement (mm)
14
12
10
8
6
4
2
0
-2
-4
-6
-8
-10
-12
-14
0
200
400
600
800
Monitor's Element Number in the Lattice
+ Uncorrected Orbit
Δ Corrected Orbit

Figure 6

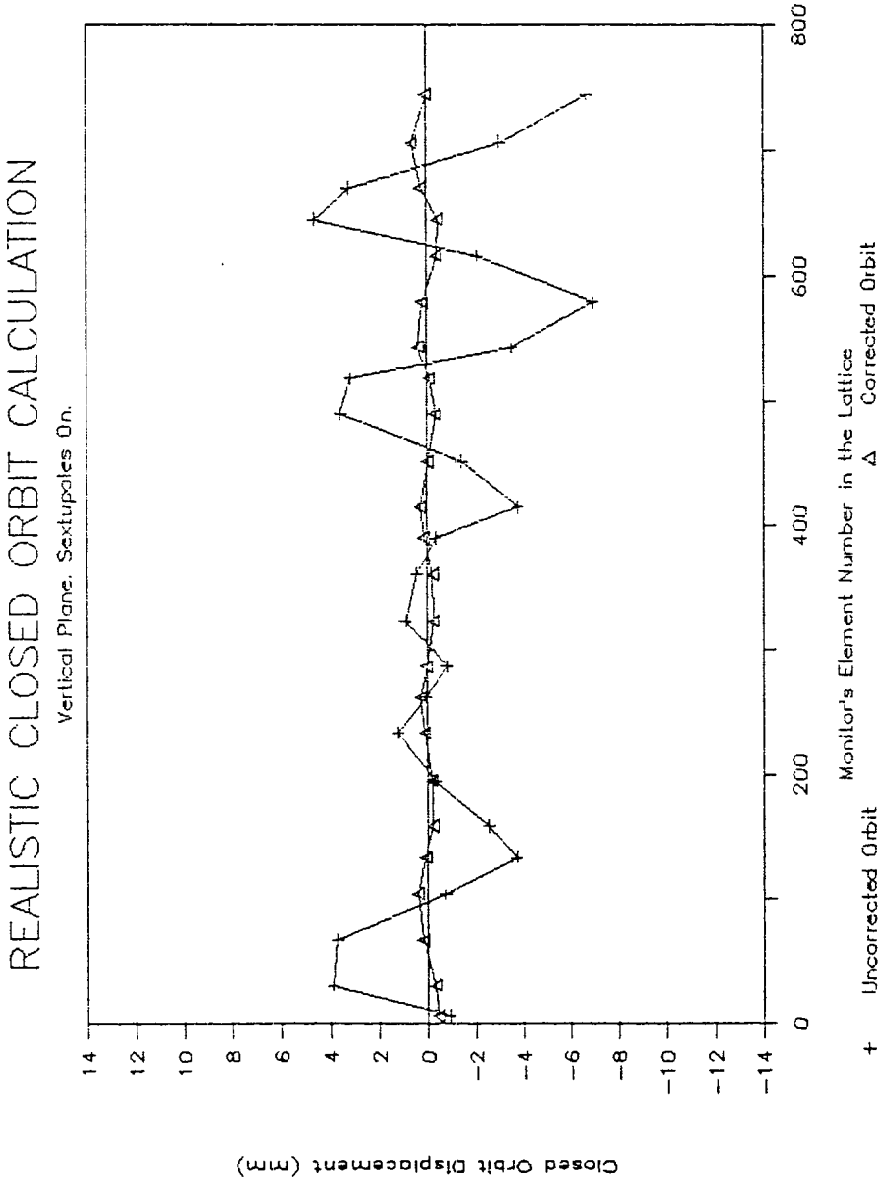
REALISTIC CLOSED ORBIT CALCULATION
Vertical Plane. Sextupoles On.
Closed Orbit Displacement (mm)
14
12
10
8
6
4
2
0
-2
-4
-6
-8
-10
-12
-14
0
200
400
600
800
Monitor's Element Number in the Lattice
+ Uncorrected Orbit
Δ Corrected Orbit